Ab Initio Molecular Orbital Study of Organometallic Complexes Containing Benzo[*b*]thiophene

Michael S. Palmer, Stuart Rowe,† and Suzanne Harris*

Department of Chemistry, University of Wyoming, Laramie, Wyoming 82071-3838

Received March 25, 1998

Ab initio molecular orbital calculations have been carried out on benzo[*b*]thiophene (BT), 2-methylbenzo[*b*]thiophene (2-MeBT), 3-methylbenzo[*b*]thiophene (3-MeBT), and a number of organometallic complexes containing these thiophenic moieties in an attempt to understand the usual preference for insertion of metal fragments into the sulfur−carbon(vinyl) bond of BT and the recent observations of insertion into the sulfur−carbon(aryl) bond. The results indicate that insertion selectivity is governed by several factors, including the orbital structure of BT, steric interactions between the metal and the heterocycle, and the metal−carbon bond strengths of the inserted products. In most cases, all three factors support the experimentally observed preference for insertion into the S−C(vinyl) bond. Subtle structural changes, however, can lead to S−C(aryl) metal-inserted products. For instance, steric factors inhibiting insertion of metal fragments into the sulfur−carbon(aryl) bond of BT can be overcome by "tied back" or relatively small metal fragments. In addition, the strength of the metal−carbon bond of the inserted product, which appears to be a determining factor leading to the otherwise unexpected sulfur−carbon(aryl) metal-inserted adducts, can be influenced by derivatizing BT or coordinating metals to the arene ring of BT.

Downloaded by CARLI CONSORTIUM on June 30, 2009
Published on July 28, 1998 on http://pubs.acs.org | doi: 10.1021/om980224e

Introduction

Although industrial hydrodesulfurization (HDS) sufficiently desulfurizes most sulfur-containing molecules, current HDS catalysts are not efficient at removing sulfur from aromatic hydrocarbons such as thiophene (T), benzothiophene (BT), or dibenzothiophene (DBT).[1] In an attempt to understand the chemistry of these heterocycles at transition-metal centers, several researchers have prepared homogeneous, organometallic complexes which serve as models for studying HDS reactions.[2−5] Many of these model complexes contain a transition-metal fragment (ML_n) which has inserted into one of the S−C bonds of a thiophenic molecule. This particular model has shown merit not only because one of the S−C bonds is broken, but also because certain metal-inserted complexes react further to desulfurize thiacycles in manners possibly related to heterogeneous HDS catalysis.[6]

An interesting feature of the metal-inserted BT complexes is that there are two different S−C bonds, S−C_v or S−C_a, into which a metal fragment may insert (C_v and C_a refer to the S-bound vinyl and aryl carbon atoms, respectively). To date, the overwhelming majority of complexes exhibit a preference for metal insertion into the S−C_v bond of the heterocycle (Chart 1).[7−12] Alternatively, metal insertion into the S−C_a bond of BT is possible but has only been observed in two systems. The first such system, (C_5Me_5)Rh(PMe_3)(η^2-*C*,*S*-2-MeC_8H_5S), was prepared via insertion of the reactive, 16-electron fragment [(C_5Me_5)Rh(PMe_3)] into 2-methylbenzothiophene (2-MeBT); the facile, reversible insertion of the rhodium fragment into 2-MeBT led to the isolation and characterization of both S−C_v and S−C_a

Chart 1

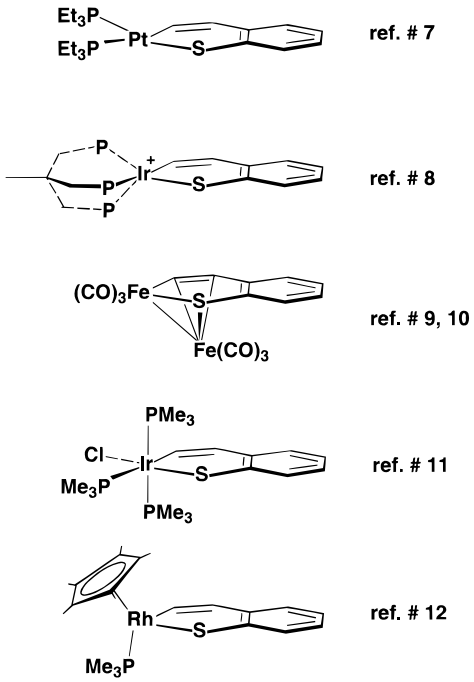

† Permanent address: Department of Chemistry, Duke University, Durham, NC 27708-0354.

(1) Topsøe, T.; Clausen, B. S.; Massoth, F. E. *Hydrotreating Catalysis*; Springer-Verlag: Berlin, 1996.
(2) Angelici, R. J. *Polyhedron* **1997**, *16*, 3073−3088.
(3) Angelici, R. J. *Coord. Chem. Rev.* **1990**, *105*, 61−76.
(4) Rauchfuss, T. B. *Prog. Inorg. Chem.* **1991**, *39*, 259−329.
(5) Sánchez-Delgado, R. A. *J. Mol. Catal.* **1994**, *86*, 287−307.
(6) Bianchini, C.; Meli, A. *J. Chem. Soc., Dalton Trans.* **1996**, 801−814.
(7) Garcia, J. J.; Mann, B. E.; Adams, H.; Bailey, N. A.; Maitlis, P. M. *J. Am. Chem. Soc.* **1995**, *117*, 2179−2186.

S0276-7333(98)00224-6 CCC: $15.00 © 1998 American Chemical Society
Publication on Web 07/28/1998

insertion products (eq 1).[13] The second system, which

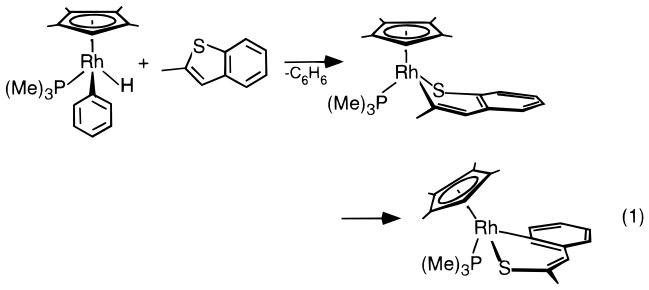

(1)

exhibits *selective* metal insertion into the S−C_a bond of BT, is a bimetallic complex containing a [$Mn(CO)_3$] moiety which is η^6-bonded to the arene portion of BT and a [$Mn(CO)_3L$] fragment (L = CO, $P(OMe)_3$, or $P(OEt)_3$) which is inserted into the S−C_a bond of the heterocycle (eq 2).[14] (An analogous η^6-BT ruthenium

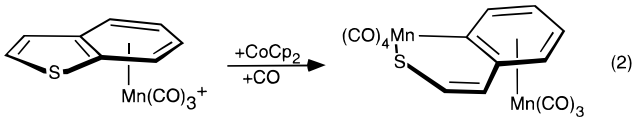

(2)

complex containing a [$Mn(CO)_4$] fragment inserted into the S−C_a bond has also been reported.)[15]

Several explanations have been offered for the preferential insertion of metals into the S−C_v bond of benzothiophene based on both experimental and theoretical data related to the proposed insertion mechanism. Studies have shown that insertion occurs for coordinatively unsaturated, electron-rich metal fragments. Experimental evidence indicates that these reactive metal centers initially coordinate to the thiophenic moiety through the sulfur atom;[16−19] insertion then proceeds via an oxidative addition of the metal. On the basis of this type of mechanism, Jones hinted that the preference for S−C_v bond insertion may be related to the character of the BT LUMO (lowest unoccupied molecular orbital), since it must be occupied upon oxidative addition. Using semiempirical calculations, he predicted a large coefficient on the vinyl carbon of the LUMO, which is indeed consistent with S−C_v insertion.[13] On the other hand, Angelici suggested that the η^1-S-bound intermediate may influence insertion by selectively weakening and thus activating the S−C_v bond. This proposal was based on the observation that the S−C_v bond of the stable S-bound complex, (C_5Me_5)$(CO)_2$Re(η^1-*S*-3-MeC_8H_5S), is lengthened approximately 0.2 Å relative to free benzothiophenes while the S−C_a bond is unaffected by complexation.[20] Finally, some researchers have noted that it may simply be sterically difficult to insert large metal nucleophiles into the more hindered S−C_a bond of BT.[7,13]

While all three of the above explanations have merit, they have not been fully examined and certainly do not account for recent observations of S−C_a-inserted products. In an attempt to understand factors leading to the observed bond selectivity of metal insertion, we have investigated electronic properties of S−C_v and S−C_a metal-inserted BT complexes and various precursors using ab initio self-consistent field molecular orbital methods. Herein we describe our initial studies which serve as a basis for understanding the preferential formation of S−C_v products. In addition, we describe an available pathway which leads to S−C_a insertion and the factors which ultimately influence the selectivity of insertion.

To address these questions, we have limited our discussion to a handful of complexes. First, we examine the results of a geometry optimization of free BT. Although both semiempirical[21−25] and ab initio[26−28] studies on BT have been reported, the primary focus of these studies has not been determining factors related to metal insertion reactions or HDS reactions in general. For the present discussion, properties such as S−C bond strengths and molecular orbital structure are examined and analyzed in terms of their influence on metal-insertion selectivity. Since many organometallic complexes containing BT incorporate derivatized heterocycles, including a number of the complexes we investigated, the electronic structures of free 2-MeBT and 3-MeBT are also examined and compared to BT. Second, we discuss the electronic structure of the stable η^1-S-BT complex (C_5Me_5)$(CO)_2$Re(η^1-*S*-3-MeC_8H_5S) in order to determine any effects on the properties of the BT moiety brought about by η^1-S complexation. For example, is the S−C_v bond activated by initial coordination through the sulfur atom? Third, we consider other factors which may affect bond activation such as steric interactions and M−C bond strengths of the inserted products. We discuss the effects each of these factors has on the rhodium-inserted complex (C_5Me_5)Rh(PMe_3)-(η^2-*C*,*S*-2-MeC_8H_5S), since it forms both kinetic S−C_v and thermodynamic S−C_a metal-inserted products, and the bimetallic systems, since they form S−C_a metal-

Downloaded by CARLI CONSORTIUM on June 30, 2009
Published on July 28, 1998 on http://pubs.acs.org | doi: 10.1021/om980224e

(8) Bianchini, C.; Meli, A.; Peruzzini, M.; Vizza, F.; Moneti, S.; Herrera, V.; Sánchez-Delgado, R. A. *J. Am. Chem. Soc.* **1994**, *116*, 4370−4381.
(9) King, R. B.; Stone, F. G. A. *J. Am. Chem. Soc.* **1960**, *82*, 4557−4562.
(10) King, R. B.; Treichel, P. M.; Stone, F. G. A. *J. Am. Chem. Soc.* **1961**, *83*, 3600−3604.
(11) Selnau, H. E.; Merola, J. S. *Organometallics* **1993**, *12*, 1583−1591.
(12) Jones, W. D.; Dong, L. *J. Am. Chem. Soc.* **1991**, *113*, 559−564.
(13) Myers, A. W.; Jones, W. D.; McClements, S. M. *J. Am. Chem. Soc.* **1995**, *117*, 11704−11709.
(14) Dullaghan, C. A.; Sun, S.; Carpenter, G. B.; Weldon, B.; Sweigart, D. A. *Angew. Chem., Int. Ed. Engl.* **1996**, *35*, 212−214.
(15) Sun, S.; Dullaghan, C. A.; Sweigart, D. A. *J. Chem. Soc., Dalton Trans.* **1996**, 4493−4507.
(16) Dong, L.; Duckett, S. B.; Ohman, K. F.; Jones, W. D. *J. Am. Chem. Soc.* **1992**, *114*, 151−160.
(17) Bianchini, C.; Jimenez, M. V.; Meli, A.; Moneti, S.; Vizza, F.; Herrera, V.; Sánchez-Delgado, R. *Organometallics* **1995**, *14*, 2342−2352.
(18) Bianchini, C.; Jimenez, M. V.; Meli, A.; Vizza, F. *Organometallics* **1995**, *14*, 3196−3202.
(19) Bianchini, C.; Herrera, V.; Jimenez, M. V.; Meli, A.; Sánchez-Delgado, R. A.; Vizza, F. *J. Am. Chem. Soc.* **1995**, *117*, 8567−8575.
(20) Choi, M.; Angelici, R. J. *Organometallics* **1992**, *11*, 3328−3334.
(21) Dewar, M. J. S.; Trinajstic′, N. *J. Am. Chem. Soc.* **1970**, *92*, 1453−1459.
(22) Geneste, P.; Guida, A.; Levache, D. *Bull. Soc. Chim. Fr.* **1982**, *11*, 136−140.
(23) Guimon, C.; Guimon, M. F.; Pfister-Guillouzo, G. *Phosphorus Sulfur* **1979**, *5*, 341−348.
(24) Ma, X.; Sakanishi, K.; Isoda, T.; Mochido, I. *Energy Fuels* **1995**, *9*, 33−37.
(25) Sánchez-Delgado, R. A.; Herrera, V.; Rincón, L.; Andriollo, A.; Martín, G. *Organometallics* **1994**, *13*, 553−516.
(26) Hinchliffe, A.; Machado, H. J. S. *J. Mol. Struct. (THEOCHEM)* **1995**, *334*, 235−242.
(27) Palmer, M. H.; Kennedy, S. M. F. *J. Chem. Soc., Perkin Trans. 2* **1974**, 1893−1903.
(28) Webber, J. S.; Woolley, R. G. *J. Mol. Struct. (THEOCHEM)* **1995**, *341*, 181−200.

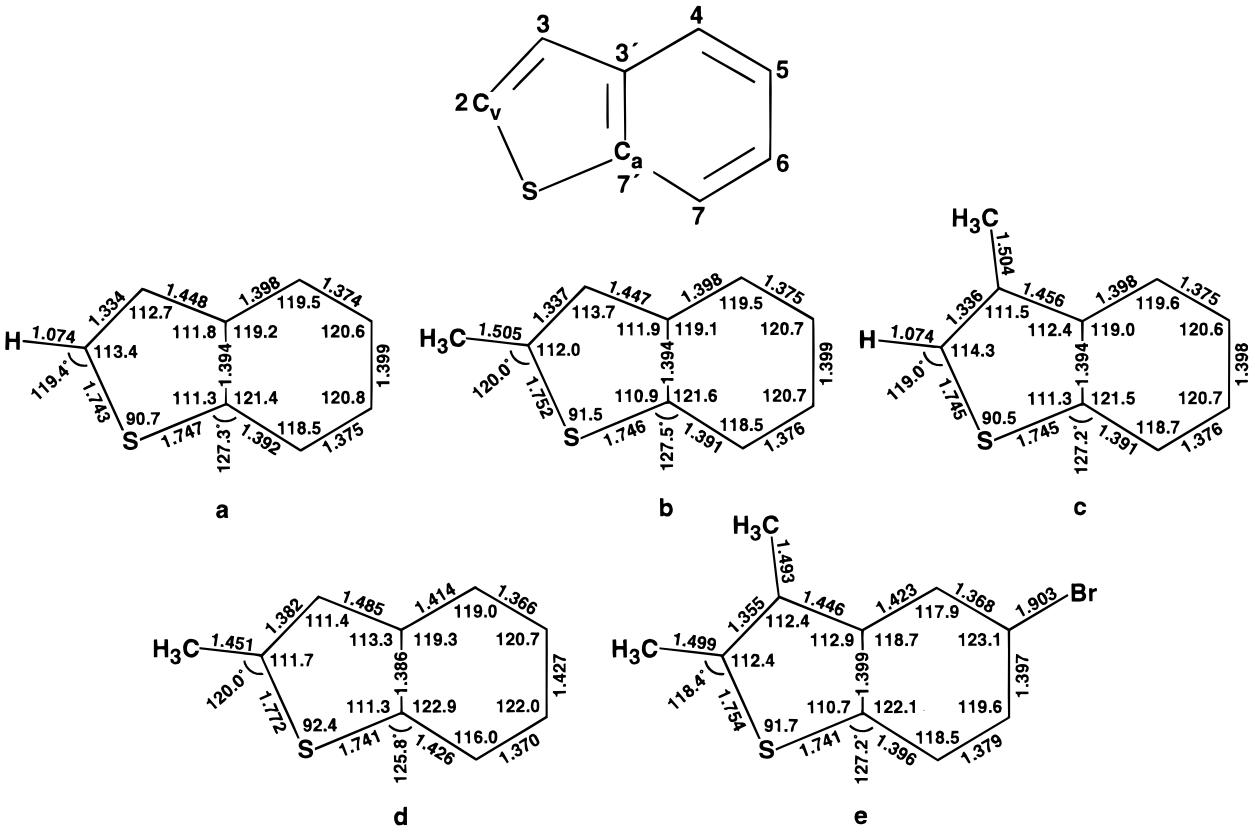

Figure 1. Calculated (HF/6-311G*) bond lengths and bond angles for (a) BT, (b) 2-MeBT, and (c) 3-MeBT. Experimental bond lengths and bond angles for the single-crystal X-ray structures of (d) 2-MeBT and (e) 5-bromo-2,3-dimethylbenzo-[*b*]thiophene.

Downloaded by CARLI CONSORTIUM on June 30, 2009
Published on July 28, 1998 on http://pubs.acs.org | doi: 10.1021/om980224e

inserted products. On the basis of the results for free BT and η^1-S-bound BT, as well as the steric and bond strength arguments, we conclude by describing the pathway which leads to both S−C_v and S−C_a products and summarize the factors which influence the stability of each adduct.

Results and Discussions

Molecular Structure of Free BT, 2-MeBT, and 3-MeBT. Bond lengths and bond angles for the HF-(Hartree−Fock)/6-311G* structure of each benzothiophene molecule studied are shown in Figure 1. Both benzo[*b*]thiophene[29] and 2-methylbenzo[*b*]thiophene[30] have been characterized by single-crystal X-ray diffraction. Unfortunately, our comparison between experimental and theoretical structures is limited to 2-MeBT as Sutherland et al. did not report coordinate data for the unsubstituted BT. Despite some unexpected features in the experimental structure of 2-MeBT, such as the long−short bond length alternation in the arene portion of the heterocycle, comparison of the crystal structure with the calculated structure shows most bond distances equivalent to 0.02 Å (the largest deviation is 0.05 Å) and bond angles equivalent to 1°. Further comparison between the single-crystal X-ray structure of 5-bromo-2,3-dimethylbenzo[*b*]thiophene,[31] which does not suffer the bond alternation observed in 2-MeBT, and the calculated structure of 2-MeBT shows even smaller differences between bond lengths and angles. On the basis of the favorable comparison between experimental and calculated structures, therefore, it is reasonable to assume that the BT and 3-MeBT structures are also accurately modeled.

Although BT, 2-MeBT, and 3-MeBT are structurally quite similar, slight differences do arise from methyl derivatization. When compared to the BT structure, 2-MeBT exhibits a slight elongation of the S−C_2 bond distance, a decrease in the S−C_2−C_3 bond angle, and an increase in the C_2−S−$C_{7'}$ and C_2−C_3−$C_{3'}$ bond angles. Similar permutations are observed for the 3-MeBT molecule; i.e., the C_3−$C_{3'}$ bond distance is lengthened, the C_2−C_3−$C_{3'}$ angle is contracted, and the S−C_2−C_3 and C_3−$C_{3'}$−$C_{7'}$ angles are expanded. These alterations in the BT structure arise from steric interactions between the methyl substituent and adjacent portions of the heterocycle. The fact that only one bond distance within the ring is lengthened implies that the methyl group interacts more strongly with certain portions of the ring system than others. Space-filling models indicate that in the case of 2-MeBT the methyl group interacts most strongly with the bulky sulfur atom and in 3-MeBT the methyl interacts most strongly with the hydrogen atom on C_4. The result is movement of the methyl substituent away from these more crowded regions.

As a final comment on structure, it is worth noting similarities in the S−C_v and S−C_a bonds. In each of the three molecules, both S−C bond distances differ by

(29) Ali-Adib, Z.; Rawas, A.; Sutherland, H. H. *Acta Crystallogr., Sect. A* **1984**, *40*, C277.
(30) Sutherland, H. H.; Rawas, A. *Acta Crystallogr., Sect. C* **1985**, *41*, 929−931.
(31) Hogg, J. H. C.; Sutherland, H. H. *Acta Crystallogr., Sect. B* **1974**, *30*, 2058−2059.

Table 1. Calculated S−C_v and S−C_a Bond Lengths and Bond Overlap Populations for BT, 2-MeBT, and 3-MeBT

		BT	2-MeBT	3-MeBT
bond length	S−C_v	1.743	1.752	1.745
	S−C_a	1.747	1.746	1.745
bond overlap population	S−C_v	0.56	0.58	0.56
	S−C_a	0.61	0.58	0.61

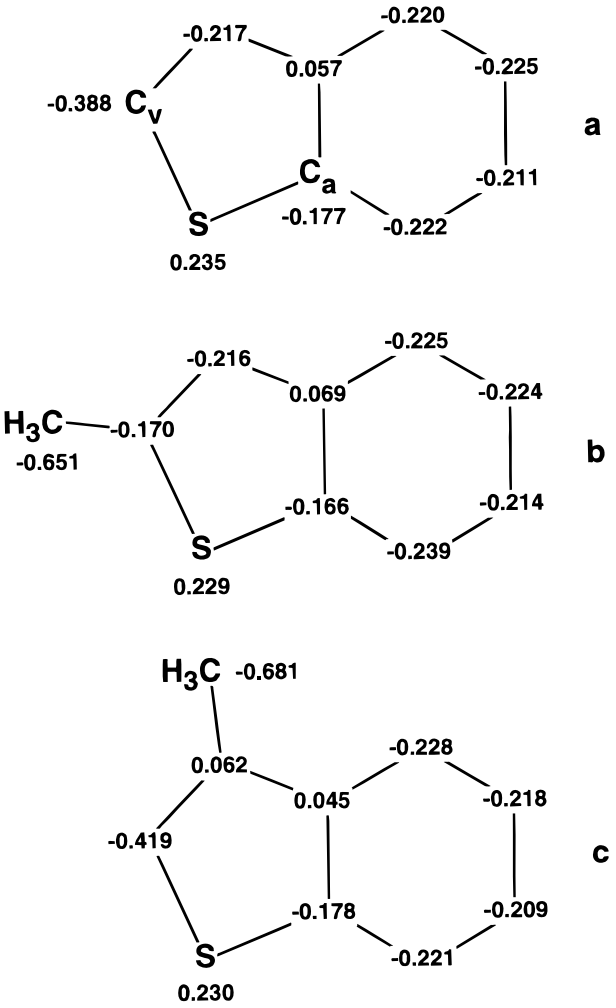

Figure 2. Calculated Mulliken charges for (a) BT, (b) 2-MeBT, and (c) 3-MeBT.

less than 0.01 Å. Bond overlap populations also suggest that the two bonds are quite similar (Table 1). Although the bond overlap populations for the S−C_a bond of BT and 3-MeBT are larger than those for the S−C_v bond, this should not be construed as an indication of increased bond strength. Mulliken population analyses merely represent a measure of bond covalency,[32,33] and the differences in bond overlap populations can be attributed to the large differences in the calculated charges on C_v and C_a (Figure 2). Taking this into account, the results suggest that there should be no insertion preference related to S−C bond strengths of the free heterocycles.

Electronic Structure of Free BT, 2-MeBT, 3-MeBT. The energy-level diagram for BT (HF/6-311G*) is shown in Figure 3. Since the compositions, relative ordering, and relative energies of the molecular orbitals

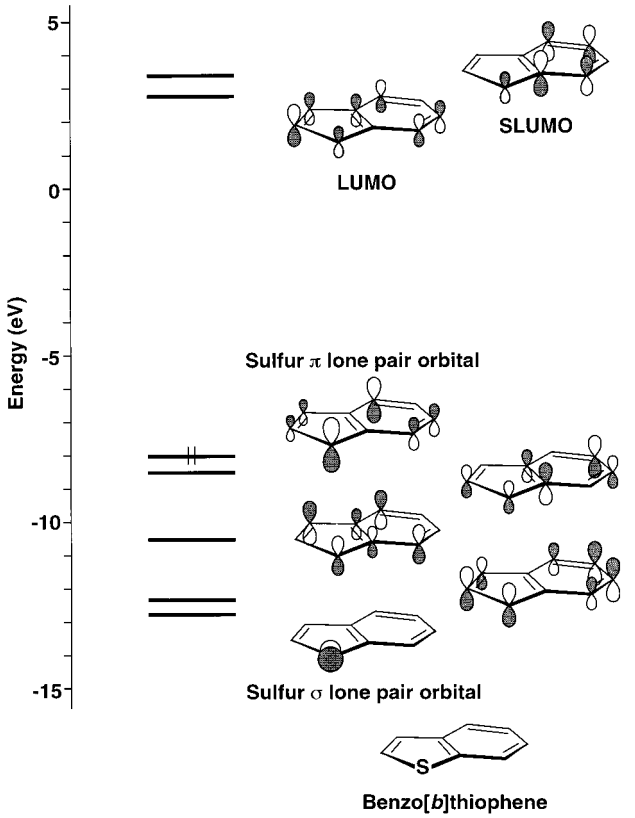

Figure 3. Calculated energy-level diagram for benzothiophene (HF/6-311G*).

of 2-MeBT and 3-MeBT are similar to those of BT, they are not shown. The frontier orbitals of BT are π orbitals with electron density lying perpendicular to the plane of the molecule. Of these, the lowest energy unoccupied molecular orbitals are of interest since the oxidative addition to electron-rich metal centers, which is characteristic of insertion, requires empty ligand orbitals. Recent calculations by Sargent indicate that the LUMO of the thiophenic moiety is particularly important due to its intimate involvement in the transition state (TS) from an η^1-S-bound complex to a metal-inserted complex; i.e., the LUMO of the thiacycle interacts with a filled metal orbital.[34] The BT LUMO is predicted to contain significant electron density on the sulfur and the vinyl carbon and an absence of density on the aryl carbon. (This is consistent with Jones's semiempirical calculation which predicted a large coefficient on the vinyl carbon.) Since the lobes on the S and C_v atoms are antibonding with respect to each other, a filled, π-type metal fragment orbital could effectively overlap with this portion of the BT LUMO. Assuming Sargent's transition-state prediction, the interaction should lead to a S−C_v insertion product (Figure 4). The orbital structure of the BT LUMO, therefore, is consistent with experimental evidence which indicates a preference for metal insertion into the S−C_v bond.

In contrast, inspection of the SLUMO (second lowest unoccupied molecular orbital) of BT reveals a concentration of electron density on the sulfur and *aryl* carbon and little density on the vinyl carbon. Similar to the LUMO, the lobes on the S and C_a atoms are antibonding with respect to each other and are available to interact

(32) Mulliken, R. S. *J. Chem. Phys.* **1955**, *23*, 1833−1840.
(33) Mulliken, R. S. *J. Chem. Phys.* **1955**, *23*, 1841−1846.
(34) Sargent, A. L.; Titus, E. P. *Organometallics* **1998**, *17*, 65−75.

Downloaded by CARLI CONSORTIUM on June 30, 2009
Published on July 28, 1998 on http://pubs.acs.org | doi: 10.1021/om980224e

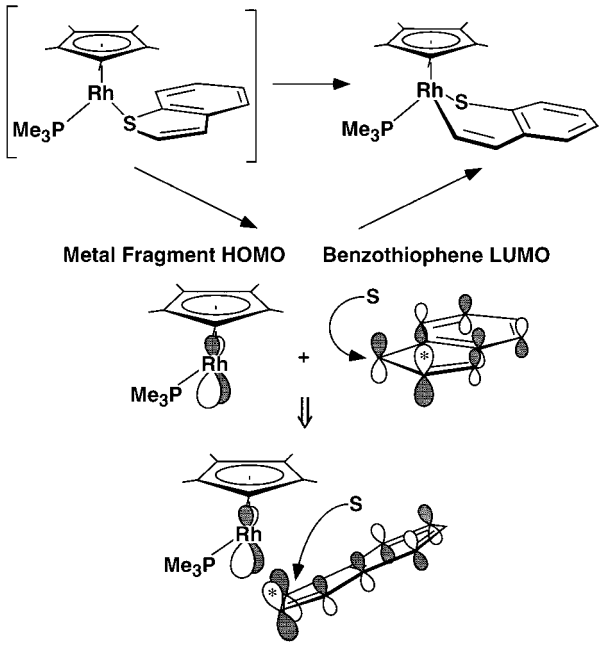

Figure 4. Probable transition state (TS) from an η^1-S-BT intermediate to a metal-inserted product based on Sargent's calculated TS for the analogous thiophene complex. The TS involves interaction between the HOMO of the metal fragment and the LUMO of the thiophenic fragment. To achieve maximum overlap with the metal orbital, the thiophene moiety rotates and tilts upward.

Table 2. Calculated Orbital Coefficients for S, C_v, and C_a in the LUMO and SLUMO of BT, 2-MeBT, and 3-MeBT

	BT	2-MeBT	3-MeBT
		LUMO	
S	−0.36	−0.44	−0.32
C_v	0.80	0.84	0.75
C_a	0.29	0.30	0.22
		SLUMO	
S	−0.36	−0.52	−0.37
C_v	0.20	0.23	0.21
C_a	0.99	1.00	1.00

with a filled metal-fragment orbital. The result of this interaction, which cannot be discounted based on similarities in the LUMO and SLUMO orbital energies, would be a S−C_a insertion product. (The *intramolecular* isomerization between S−C_v and S−C_a products of the rhodium-inserted complex $(C_5Me_5)Rh(PMe_3)(\eta^2\text{-}C,S\text{-}2\text{-}MeC_8H_5S)$ offers experimental support for a small LUMO/SLUMO gap.) The SLUMO, consequently, provides a viable alternative to a nucleophilic metal when, for whatever reason, formation of a S−C_v insertion product is unfavorable. Similar orbital characters are also observed for the LUMO and SLUMO of 2- and 3-MeBT (Table 2).

In summary, the possibility for the existence of two different metal-inserted BT products stems directly from the orbital structure of the BT LUMO and SLUMO. Preferential insertion into the S−C_v bond can be attributed in part to the large sulfur and vinyl carbon contributions to the LUMO. Because of the small energy difference between the LUMO and SLUMO, however, instability in the S−C_v adduct can lead to an alternative metal-inserted product. The significant sulfur and aryl carbon content of the SLUMO would result in a S−C_a metal-inserted product. Finally, although these results are consistent with the observed preference for S−C_v bond cleavage, the narrow LUMO/SLUMO gap suggests that the preference for occupying either orbital is small, indicating that factors other than the orbital structure of BT could also contribute to the bond insertion selectivity.

$(C_5Me_5)(CO)_2Re(\eta^1\text{-}S\text{-}3\text{-}MeC_8H_5S)$. The results of the calculations on free BT clearly provide a basis for understanding the observance of two different metal-inserted products and suggest at least one reason for the preferential activation of the S−C_v bond. Since metal insertion into a S−C bond is preceded by η^1-S coordination of the thiophenic species, however, it is useful to understand any structural or electronic effects introduced into the BT moiety by initial complexation to a transition metal. For instance, does the η^1-S bonding mode of BT selectively weaken the S−C_v bond of the thiacycle or does the orbital structure of the BT moiety change dramatically when coordinated? To address these questions, we have investigated the electronic structure of the stable η^1-S-BT complex $(C_5Me_5)(CO)_2Re(\eta^1\text{-}S\text{-}3\text{-}MeC_8H_5S)$.

As mentioned earlier, structural characterization of $(C_5Me_5)(CO)_2Re(\eta^1\text{-}S\text{-}3\text{-}MeC_8H_5S)$ revealed an elongation of the S−C_v bond distance of the heterocycle upon ligation while the S−C_a bond length was unaffected. Not surprisingly, this led to the conclusion that the η^1-S bonding mode of BT selectively weakens and, therefore, activates the S−C_v bond toward insertion. On the surface, it seems reasonable to rationalize this observation in terms of electronic factors associated with metal coordination; i.e., ligand to metal donation could depopulate BT orbitals which are S−C_v bonding or metal to ligand back-donation could populate empty ligand orbitals which are S−C_v antibonding. Both would lead to elongation of the S−C_v bond. Calculations show that the BT sulfur σ orbital (see Figure 3) and HOMO are the only ligand orbitals significantly involved in donation to the metal. Depopulation of either orbital is not expected to lengthen the S−C_v bond since both orbitals are predominantly sulfur lone pair orbitals. On the other hand, calculations indicate that metal to ligand back-donation is not appreciable for this complex, and therefore, occupation of antibonding orbitals also cannot account for the observed alteration of structure. Previous calculations on S-bound thiophene and dibenzothiophene complexes are in complete agreement with the above results; i.e., ligand donation stems primarily from sulfur lone pair orbitals and metal back-bonding is generally small.[35,36] The fact that *no* perturbation in the structure of the heterocycles for the T and DBT systems has been observed prompted us to calculate a fully optimized structure of $(C_5Me_5)(CO)_2Re(\eta^1\text{-}S\text{-}3\text{-}MeC_8H_5S)$. Relative to the experimental structure, the optimized structure shows a contraction of the S−C_v bond length to a value characteristic of free 3-MeBT, 1.75 Å, further contradicting the notion that S-bound coordination leads to S−C_v bond activation. Consequently, the theoretical evidence and the fact that other anomalies in the $(C_5Me_5)(CO)_2Re(\eta^1\text{-}S\text{-}3\text{-}MeC_8H_5S)$ struc-

(35) Harris, S. *Organometallics* **1994**, *13*, 2628−2640.
(36) Harris, S. *Polyhedron* **1997**, *16*, 3219−3233.

Downloaded by CARLI CONSORTIUM on June 30, 2009
Published on July 28, 1998 on http://pubs.acs.org | doi: 10.1021/om980224e

Downloaded by CARLI CONSORTIUM on June 30, 2009
Published on July 28, 1998 on http://pubs.acs.org | doi: 10.1021/om980224e

ture exist[37] suggest that bond activation as a general, intrinsic property of η^1-S coordination should be considered with caution until other S-bound BT complexes are structurally characterized.

Assuming that S−C_v bond activation is not associated with η^1-S coordination, we analyzed the electronic structure of the optimized $(C_5Me_5)(CO)_2Re(\eta^1$-*S*-3-$MeC_8H_5S)$ in order to examine the orbital structure of the bound thiophene ligand. The calculations reveal that the LUMO and SLUMO of the complex are primarily BT in character and correspond to the LUMO and SLUMO of the free BT ligand, respectively. That is, the molecular orbitals leading to S−C_v and S−C_a insertion remain the lowest energy, empty orbitals. Both orbitals remain energetically accessible with only a small energy gap between them; metal insertion into the S−C_v bond is still expected to be slightly favored over S−C_a insertion. The arguments concerning insertion trends which we proposed for free BT, therefore, remain valid for the complexed ligand.

On the basis of these results, it is clear that bond activation is not associated with initial η^1-S coordination of BT and does not play a role in insertion selectivity. To this juncture, the only evidence presented which is suggestive of a S−C bond insertion preference is the orbital structure of BT. As we pointed out, however, the energy gap between the BT LUMO, which leads to S−C_v insertion, and the SLUMO, which leads to S−C_a insertion, is narrow enough that orbital structure alone cannot be considered a dominant factor governing the stability of the insertion product. To fully account for the observed preference for metal insertion into the S−C_v bond, steric interactions and metal−carbon bond strengths must also be considered.

Steric Interactions. Numerous examples exist in which steric interactions play some role in the insertion of metals into thiophenes. For example, Jones has shown that reaction of the 16-electron fragment $[(C_5Me_5)Rh(PMe_3)]$ with 2-methylthiophene results in selective insertion into the less hindered, nonalkylated S−C bond.[12] This tendency for insertion to occur away from ring substituents has been observed in a number of thiophene complexes as well as alkylated dibenzothiophene systems.[18,38−42] Steric interactions have also been shown to play an important role in the configuration of the ring systems in a number of metal-inserted thiophene complexes. We have reported that the distortions observed in the metallacycles of various systems can be virtually eliminated by removal or reduction of sterically demanding ligands.[43] With these observations

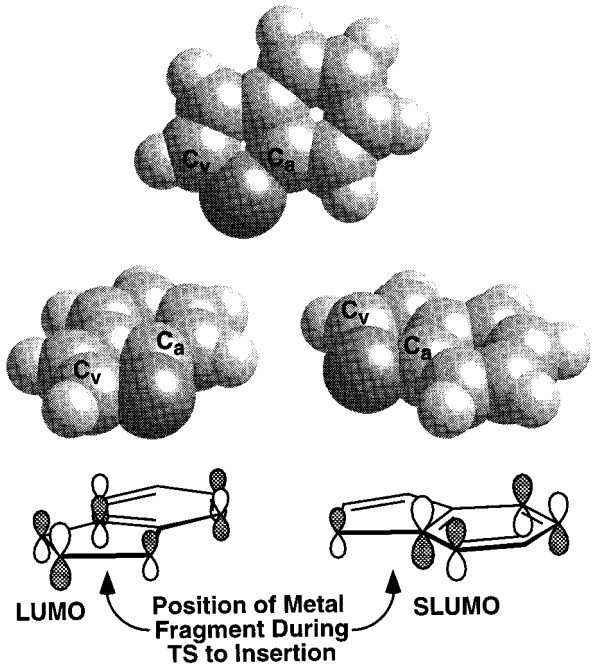

Figure 5. Space-filling representations of BT illustrating steric interactions associated with metal insertion into a S−C bond. Orbital overlap between a filled metal fragment orbital and BT LUMO and subsequent insertion into the S−C_v bond by the metal fragment is not hampered by steric interactions, whereas overlap with the SLUMO and insertion into the S−C_a bond is restricted by the H atom on C_7 of the thiacycle.

in mind, it is not unreasonable to assume that steric interactions also play a role in determining the insertion selectivity of metal-inserted BT complexes.

On the basis of regioselectivity arguments, insertion into a S−C bond of BT should be selective toward the less sterically hindered bond. Inspection of the calculated structure of BT reveals that although the S−C_a bond is more open than the S−C_v bond in terms of nearest neighbor atoms (127.3° vs 119.4°), access is somewhat hindered due to the protruding H atom on C_7 of the arene ring (Figure 5). The obstructive nature of the ring is magnified if one takes into consideration the fact that the BT moiety most rotate toward C_a during the TS from an S-bound intermediate to a S−C_a metal-inserted product in order to enhance metal−ligand overlap. Because the majority of metal-inserted BT complexes contain bulky metal fragments incorporating large, alkyl-substituted phosphine ligands (see Chart 1), insertion into the S−C_a bond is expected to be quite difficult in terms of this steric interaction. The S−C_v bond, on the other hand, is relatively unencumbered and provides for a more accessible insertion site. Increasing the steric bulk at C_v, however, could influence the ease of insertion into the vinyl bond.

Clearly, insertion of large metal fragments into the S−C_a bond of BT cannot be totally discounted since insertions of these fragments are known to occur into the analogous S−C_a bond of *di*benzothiophene.[7,17] Nevertheless, insertion into the S−C_v bond of BT should be preferred for large nucleophiles when based solely on steric arguments. Only when the inserting metal fragment is "tied back" as in $(C_5Me_5)Rh(PMe_3)(\eta^2$-*C*,*S*-2-$MeC_8H_5S)$ or comparatively small as in the case of the

(37) Other anomalies in the structure of $(C_5Me_5)(CO)_2Re(\eta^1$-*S*-3-$MeC_8H_5S)$ reinforce our suggestion that the elongated S−C_v bond is an experimental artifact rather than a real observable. For instance, considerable differences in the C−C bond lengths exist in the arene ring of the heterocycle. The fact that the hydrogen atoms were not included in the model may account for some of the discrepancies.

(38) Buys, I. E.; Field, L. D.; Hambly, T. W.; McQueen, A. E. D. *J. Chem. Soc., Chem. Commun.* **1994**, 557−558.
(39) Garcia, J. J.; Arevalo, A.; Capella, S.; Chehata, A.; Herdandez, M.; Montiel, V.; Picazo, G.; Rio, F. D.; Toscano, R. A.; Adams, H.; Maitlis, P. M. *Polyhedron* **1997**, *16*, 3185−3195.
(40) Jones, W. D.; Vicic, D. A.; Chin, R. M.; Roache, J. H.; Myers, A. W. *Polyhedron* **1997**, *16*, 3115−3128.
(41) Myers, A. W.; Jones, W. D. *Organometallics* **1996**, *15*, 2905−2917.
(42) Dullaghan, C. A.; Carpenter, G. B.; Sweigart, D. A. *Organometallics* **1997**, *16*, 5688−5695.
(43) Blonski, C.; Myers, A. W.; Palmer, M.; Harris, S.; Jones, W. D. *Organometallics* **1997**, *16*, 3819−3827.

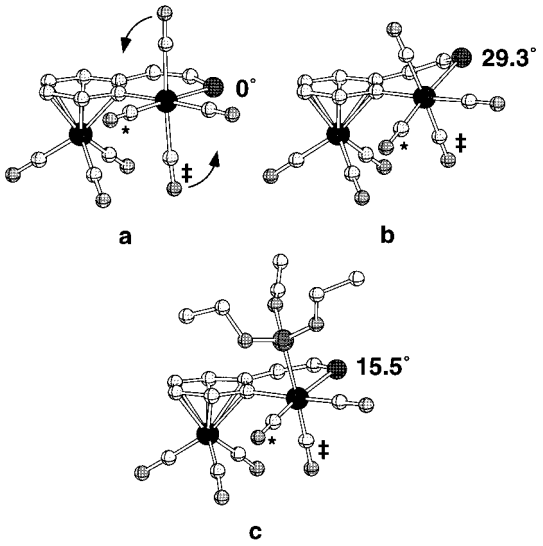

Figure 6. Steric interactions present in bimetallic manganese-inserted BT complexes. Complex **a** represents an idealized structure assuming no steric interactions; **b** is the crystal structure of the tetracarbonyl product; **c** is the crystal structure of the $P(OEt)_3$-substituted complex. Two of the carbonyl ligands are labeled for identification purposes. The angles refer to the position of the sulfur atom relative to the plane of the arene portion of the heterocycle.

bimetallic manganese systems can steric interactions which hinder $S-C_a$ insertion be overcome.

It is worth noting that even though small metal nucleophiles such as $[Mn(CO)_4]$ are capable of inserting into the $S-C_a$ bond of BT, the resulting structure remains dependent on a number of steric interactions, including those between the metal fragment and the arene ring of the heterocycle. These interactions for the bimetallic manganese complex are shown in Figure 6. If one assumes no steric controls to be present, the opened BT moiety would be expected to remain planar with the inserted manganese octahedrally coordinated (Figure 6a). Inspection of the crystal structure (Figure 6b),[14] however, reveals a counterclockwise rotation of the $[Mn(CO)_4]$ fragment. The rotation leads to a distortion of the heterocycle since the octahedral environment of the inserted manganese atom is preserved in order for the metal to effectively interact with the four carbonyl ligands. Space-filling models of the structure shown in Figure 6a as well as molecular mechanics calculations on the structure indicate steric interactions between CO* and the H atom on C_7 of the arene ring and between $CO^{\ddagger}$ and the carbonyl ligands of the piano stool. Rotation of the $[Mn(CO)_4]$ fragment reduces both of these interactions. The degree of rotation, though, is restricted by steric interactions between the upper axial CO of the $[Mn(CO)_4]$ moiety and the ring system. Substitution of the axial CO with $P(OEt)_3$ limits the degree of rotation of the $[Mn(CO)_4]$ fragment due to repulsions from the ring system and thereby reduces the distortion of the metallacycle. This is observed in the crystal structure of the $P(OEt)_3$-substituted complex (Figure 6c)[14] where the sulfur atom is only lifted 15.5° out of the plane of the heterocycle while the sulfur atom in the CO derivative is lifted 29.3°.

The steric interactions described above are magnified if the H atom on C_7 is substituted with either a methyl or ethyl group (Figure 7a). In fact, interactions with

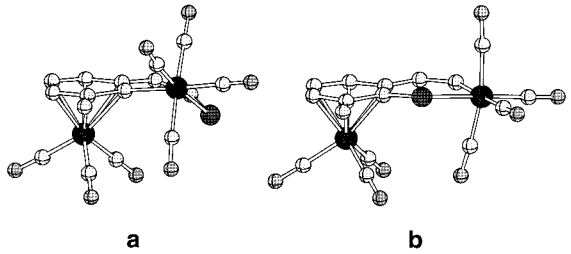

Figure 7. Experimental structures of the products obtained from the insertion of $[Mn(CO)_4]$ into the $S-C$ bonds of $[(\eta^6\text{-7-MeBT})Mn(CO)_3]^+$; (a) is the kinetic $S-C_a$ insertion product, and (b) is the thermodynamic $S-C_v$ insertion product.

the alkyl group are so severe that isomerization to a $S-C_v$-inserted product is observed; the experimental structure of the vinyl-inserted adduct shows no signs of deformation due to steric factors (Figure 7b).[44] Consequently, it is somewhat surprising that insertion of the small $[Mn(CO)_4]$ fragment into BT is selective toward the $S-C_a$ bond when the $S-C_v$ bond is more accessible and leads to fewer steric interactions. The selectivity in this particular system, therefore, must be accounted for by another factor.

Metal−Carbon Bond Strengths. Work in areas of hydrocarbon activation has led to the observation that the strength of C−H bonds are directly related to their activity. Interestingly, stronger bonds are more easily activated than weaker ones. Jones and Feher explained this trend in terms of the strength of the resultant metal−carbon bond; i.e., activation of the strongest C−H bond results in formation of the strongest M−C bond (eq 3, X = H or M).[45] Consequently, when Jones

$$\underset{\text{(phenyl)}}{X\text{—}C_6H_5} > \underset{\text{(vinyl)}}{X\text{—}CHCH_2} > \underset{\text{(methyl)}}{X\text{—}CH_3} > \underset{(1^\circ)}{X\text{—}CH_2R} > \underset{(2^\circ)}{X\text{—}CHR_2} >$$

$$\underset{(3^\circ)}{X\text{—}CR_3} > \underset{\text{(benzyl)}}{X\text{—}CH_2(C_6H_5)} > \underset{\text{(allyl)}}{X\text{—}CH_2CHCH_2} \qquad (3)$$

observed both $S-C_v$ and $S-C_a$ insertion products of $(C_5Me_5)Rh(PMe_3)(\eta^2\text{-}C,S\text{-}2\text{-}MeC_8H_5S)$, he concluded that the thermodynamic stability of the $S-C_a$ isomer is attributed to formation of a stronger metal−aryl bond.[13] Unfortunately, Jones's conclusion is based on general features about M−C bond strengths roughly determined through experiment rather than more quantitative measurements.

In light of the ever-increasing data regarding the relationship between bond strength and bond activation, consideration should be given to the idea that M−C bond strengths can affect insertion selectivities. To do so, however, requires a more objective means of evaluating and comparing bond strengths. In a recent theoretical study by Seigbahn, a systematic investigation of factors influencing M−C bond strengths for the series of second-row transition-metal atoms was undertaken.[46] He found, in agreement with the ordering shown in eq 3, that M−C bond strengths increase with decreasing hybridization ($M-C_{sp^3} < M-C_{sp^2} < M-C_{sp}$), decreasing substitution at the metal-bound carbon (M−

(44) Dullaghan, C. A.; Zhang, X.; Walther, D.; Carpenter, G. B.; Sweigart, D. A. *Organometallics* **1997**, *16*, 5604−5606.
(45) Jones, W. D.; Feher, F. J. *Acc. Chem. Res.* **1989**, *22*, 91−100.
(46) Siegbahn, P. E. M. *J. Phys. Chem.* **1995**, *99*, 12723−12729.

Downloaded by CARLI CONSORTIUM on June 30, 2009
Published on July 28, 1998 on http://pubs.acs.org | doi: 10.1021/om980224e

Chart 2

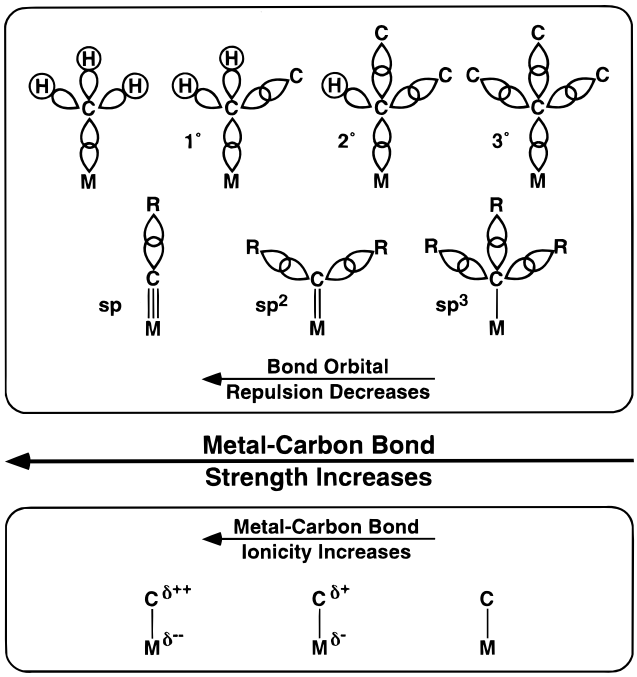

$C_3° < M-C_2° < M-C_1°$), and decreasing alkyl chain length. On the basis of these general trends and the supporting numerical data, Seigbahn concluded that the strength of a M−C bond is heavily dependent on both the ionic contribution to the bond and the repulsive interactions between M−C and C−substituent bonding orbitals. (To illustrate repulsive interactions between bonding orbitals, consider interactions between a M−C bond and a C−H or $C-CH_3$ bond. Greater electron density resides in the bonding region of the carbon−methyl bond compared to the carbon−hydrogen bond. Consequently, the $C-CH_3$ bonding orbitals generate a greater repulsive interaction with M−C bonding orbitals. This leads to weakening of the M−C bond. Jones has also commented on the effects of this type of repulsive interaction on metal−carbon bond strengths.)[45] Any factor which increases the ionicity of the bond or reduces repulsive interactions between bonding orbitals will lead to a stronger bond (Chart 2). (Seigbahn discounted other possible explanations for the bond strength trends such as the stability of the hydrocarbon free radical and the amount of s-character in a hybrid since neither account for the relatively stronger M−C bonds when compared to their C−H counterparts. In addition, he found little evidence of π-bonding interactions affecting the bond strengths.) Although Seigbahn is careful to note that it is difficult to separate the ionic and repulsive components and quantify their individual roles in the resultant bond strength, their respective influence on the bond is expected to vary predictably. For example, the ionic contribution to the bond strength may become large in systems where the charge on the metal is positive, and repulsive interactions may be more important when the metal charge is negative. Thus, measures of ionicity and repulsive interactions become particularly useful for predicting relative M−C bond strengths when applied to similar systems, as in the case of metal-inserted BT complexes, and they provide a quantitative means for examining Jones's suggestion that insertion into the $S-C_a$ bond of 2-MeBT is promoted by formation of the stronger $M-C_a$ bond.

Table 3. Calculated Mulliken Charges for S, C_v, and C_a in BT, 2-MeBT, and 3-MeBT

	BT	2-MeBT	3-MeBT
S	0.24	0.23	0.23
C_v	−0.39	−0.17	−0.42
C_a	−0.18	−0.17	−0.18

Table 4. Calculated Mulliken Charges for Rh and the Metal-Bound Carbon Atom in $S-C_v$ and $S-C_a$ [$(C_5Me_5)Rh(PMe_3)$]-Inserted BT and 2-MeBT Complexes

	BT		2-MeBT	
	$S-C_v$	$S-C_a$	$S-C_v$	$S-C_a$
Rh	0.22	0.29	0.20	0.29
C	−0.51	−0.35	−0.27	−0.36
$\Delta(Rh-C)$[a]	0.73	0.64	0.47	0.65

[a] Arithmetic difference between the Rh and metal-bound C charges.

Since both the vinyl and aryl carbon atoms in benzothiophenes are sp^2 hybridized, the only factor which influences the repulsive interactions is the degree of substitution at the metal-bound carbon. In BT and 3-MeBT, C_v is bound to one sp^2 carbon and one hydrogen atom while C_a is bound to two sp^2 carbon atoms. In 2-MeBT, C_v is bound to one sp^2 carbon and one sp^3 carbon atom and C_a remains bound to two sp^2 carbon atoms. Repulsive interactions, therefore, are expected to be the least for the $M-C_v$ bond in the case of BT and 3-MeBT and the least for the $M-C_a$ in the case of 2-MeBT. The ionic contribution to the bond strength can be best analyzed through calculated Mulliken charges of the vinyl and aryl carbon atoms of the heterocycles (Table 3). (Although Mulliken analysis does not explicitly account for ionic bonding interactions, Mulliken charges do indicate the relative ionicity of a bond.) The charges indicate that the more ionic M−C bond will be formed with the vinyl carbon for BT and 3-MeBT. On the other hand, the methyl group of 2-MeBT delocalizes the negative charge on C_v and leads to similar charges on both carbon atoms. The combined results, taking into consideration both repulsive interactions and ionicity arguments, suggest that the strongest bonds will be formed between the metal and vinyl carbon in BT and 3-MeBT and metal and aryl carbon in 2-MeBT.

While the results seem to contradict experimental observations that M−aryl bonds are in general stronger that M−vinyl bonds, this may simply be a consequence of the less than ideal nature of these heterocyclic systems. Evidence for the reversal in the bond strength trend is provided by the calculated charges of metal and carbon atoms for a series of $[(C_5Me_5)Rh(PMe_3)]$-inserted BT and 2-MeBT complexes (Table 4). Insertion into BT forms a more ionic and presumably stronger $Rh-C_v$ bond, while insertion into 2-MeBT forms a more ionic $Rh-C_a$ bond. This result is reflected in the *selective* insertion of $[(C_5Me_5)Rh(PMe_3)]$ into the $S-C_v$ of BT.[12] Only when the rhodium fragment is reacted with 2-MeBT is the $S-C_a$ product observed.

Downloaded by CARLI CONSORTIUM on June 30, 2009
Published on July 28, 1998 on http://pubs.acs.org | doi: 10.1021/om980224e

Downloaded by CARLI CONSORTIUM on June 30, 2009
Published on July 28, 1998 on http://pubs.acs.org | doi: 10.1021/om980224e

As a final comment on the [(C_5Me_5)Rh(PMe_3)]-inserted 2-MeBT isomers, it is interesting to consider why both insertion products are observed. Two separate factors must be considered in order to understand the initial activation of the S−C_v bond. First, recall that the orbital structure of the 2-MeBT LUMO contains orbital density on the S and C_v atoms which favors insertion into the S−C_v bond. Second, although the two S−C bonds of 2-MeBT are virtually identical with respect to bond lengths and bond overlap populations, the bonds differ in their local, structural environments. The environment affects the access metal fragments have to the bonds; the methyl group on C_v hinders access to the S−C_v bond, and the hydrogen atom on C_7 of the heterocycle limits access to the S−C_a bond. The fact that every example of insertion into 2-MeBT shows initial activation of the S−C_v bond suggests, in general, that the methyl group restricts insertion to a lesser extent than the hydrogen atom on C_7 or that, at the very least, the differences are negligible such that the nature of the 2-MeBT LUMO becomes the dominant factor governing the selectivity. Because the [(C_5Me_5)Rh-(PMe_3)] fragment has a relatively open, tied back structure, the steric hindrances to insertion are expected to be small and the initial preference for insertion of the metal fragment into the S−C_v bond of 2-MeBT is best explained in terms of the orbital structure of 2-MeBT.

In an earlier publication, we suggested that steric interactions between the methyl group and the *inserted* metal fragment may be responsible for the observed isomerization. More rigorous calculations indicate, however, that sterics actually play a minor role in the transformation. This is mostly due to the ability of the ring system to distort, causing a significant reduction in steric strain while having minimal impact on the electronic structure of the system. The presence of the methyl group, however, does lead to repulsive interactions between Rh−C_v and C_v−CH_3 bonding orbitals. The result is a weakening of the Rh−C_v bond, reflected in the smaller difference between the Rh and C charges (0.47 vs 0.65 for the Rh−C_a bond) and isomerization to the thermodynamic S−C_a metal-inserted product.

Somewhat analogous behavior has been observed by Bianchini and co-workers while investigating the insertion of the iridium fragment [(triphos)IrH] (triphos = $MeC(CH_2PPh_2)_3$) into 2-MeBT.[47] Consistent with Jones's rhodium system, initial insertion occurs into the S−C_v bond. However, no conversion to a S−C_a product was observed, even though the Ir−C_v bond is predicted to be fairly weak due to repulsive interactions between Ir−C_v and C_v−CH_3 bonding orbitals. In fact, the repulsive interactions are expected to be significantly greater in this system when compared to the rhodium complex since large, negative iridium charges have been calculated for similar [(triphos)Ir]-inserted thiophenic complexes.[48] The extreme bulk of the triphos ligand, however, precludes insertion into the S−C_a bond of 2-MeBT. Rather than converting to a S−C_a adduct, the strong repulsive interactions leading to the weakened Ir−C_v bond are removed by rearrangement to an η^3-

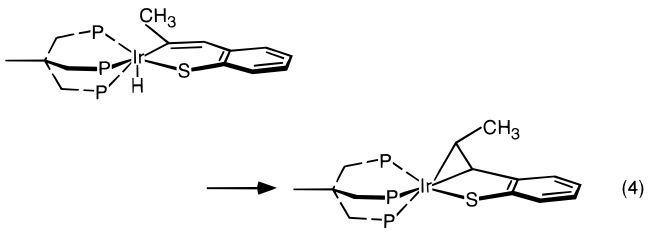

(4)

bound BT complex (eq 4). This structural configuration not only reduces repulsive interactions between bonding orbitals and steric interactions between the ring methyl and the metal fragment, but also provides a mechanism for the removal of electron density from the highly negatively charged iridium center via metal-to-olefin π-back-bonding.

The strength of the resultant M−C bond may also play a significant role in the selective insertion of [Mn-$(CO)_4$] into the S−C_a bond of the bimetallic systems. Although little is currently known about the activation/insertion mechanism of these unique systems, preliminary calculations on the [(η^6-BT)$Mn(CO)_3$]$^+$ and the [(η^6-BT)Ru(η^6-benzene)]$^{2+}$ precursors as well as [(η^6-BT)Ru(η^5-C_5H_5)]$^+$ were carried out using nonempirical, approximate Hartree−Fock, Fenske−Hall molecular orbital methods.[49] The calculations reveal that precoordination has a minimal effect on the compositions and the relative energies of the molecular orbitals important to metal insertion. As such, insertion into the S−C_v bond of the η^6-bound BT species is still *slightly* favored over insertion into the aryl bond. More importantly, the calculations also indicate that η^6-coordination of metal fragments to the arene portion of benzothiophene leads to a reversal in the calculated charges on C_v and C_a. Table 5 compares charges on the S-bound carbon atoms in both free and η^6-coordinated BT complexes. (See Calculational Details for specifics on the structures utilized for the single-point Fenske−Hall calculations.) Inspection shows that C_v is the most negative of the two carbon atoms for free BT molecules and C_a is the most negative for η^6-coordinated complexes. This suggests that precoordination leads to a more ionic and thus stronger M−C_a bond. Formation of a stronger M−C_a bond could account for the selective insertion of [Mn-$(CO)_4$] into the S−C_a bond despite preferences based on the orbital structure of BT and steric interactions associated with the S−C_a bond. While results at the Fenske−Hall level of theory are not directly comparable to the ab initio results, correlation of electronic structure and properties between the two methods is quite good. In fact, all of the ab initio calculations described within this report were also calculated at the Fenske−Hall level and the results are consistent in every aspect. Consequently, we are confident that the reversal in charges observed for the η^6-bound BT complexes are accurate. Nevertheless, as part of a more thorough investigation of the bimetallic manganese systems, we expect to confirm the effects precoordination has on the C_v and C_a charges and the corresponding metal−carbon bond strengths using higher levels of theory.

Summary

The possibility for the existence of two different metal-inserted BT products stems directly from the orbital

(47) Bianchini, C.; Casares, J. A.; Masi, D.; Meli, A.; Pohl, W.; Vizza, F. *J. Organomet. Chem.* **1997**, *541*, 143−155.
(48) Palmer, M.; Carter, K.; Harris, S. *Organometallics* **1997**, *16*, 2448−2459.
(49) Hall, M. B.; Fenske, R. F. *Inorg. Chem.* **1972**, *11*, 768−775.

Table 5. Calculated Mulliken Charges (Fenske−Hall) for C_v and C_a in BT, 3-MeBT, $[(\eta^6\text{-BT})Mn(CO)_3]^+$, $[(\eta^6\text{-BT})Ru(\eta^6\text{-benzene})]^{2+}$, and $[(\eta^6\text{-BT})Ru(\eta^5\text{-}C_5H_5)]^+$

	C_v	C_a
BT	−0.017	0.023
3-MeBT	−0.067	0.034
$[(\eta^6\text{-BT})Mn(CO)_3]^+$	0.019	−0.017
$[(\eta^6\text{-BT})Ru(\eta^6\text{-benzene})]^{2+}$	0.053	−0.038
$[(\eta^6\text{-BT})Ru(\eta^5\text{-}C_5H_5)]^+$	0.079	−0.016

structure of the BT LUMO and SLUMO. On the basis of Sargent's predicted insertion mechanism, the character of the LUMO is consistent with S−C_v insertion while the character of the SLUMO coincides with S−C_a insertion. While occupation of the LUMO is energetically preferred, the calculated LUMO/SLUMO gap is small; the small gap is consistent with the *intramolecular* pathway between the S−C_v and S−C_a products of the rhodium-inserted complex $(C_5Me_5)Rh(PMe_3)(\eta^2\text{-}C,S\text{-}2\text{-}MeC_8H_5S)$. Occupation of the SLUMO, therefore, is readily achievable.

Initial η^1-S coordination of the BT to a transition metal has a minimal effect on the atomic and electronic structure of the ligand. Our theoretical evidence for $(C_5Me_5)(CO)_2Re(\eta^1\text{-}S\text{-}3\text{-}MeC_8H_5S)$ and previous theoretical and experimental evidence for η^1-S T and DBT complexes suggest that the S−C_v bond is unaffected and certainly not activated by initial coordination through the sulfur atom. In addition, the orbital structure of the ligand persists upon complexation and the BT molecular orbitals responsible for S−C_v and S−C_a insertion products become the LUMO and SLUMO of the complex.

In all cases, steric factors favor insertion into the S−C_v bond since the alternative S−C_a bond is hindered by unfavorable interactions between the inserting metal fragment and the arene portion of the heterocycle. Although steric inhibition associated with S−C_a insertion can be overcome if the inserting metal fragment is either tied back, as in the case of the rhodium complex, or relatively small, as in the bimetallic systems, there remain significant steric interactions between the metal fragment and arene moiety of the BT ligand. Thus, steric arguments alone cannot account for the observed insertion of metal fragments into the S−C_a bond of BT.

When steric interactions do not limit access to either the S−C_v or S−C_a bond, the factor most affecting the stability of a metal-inserted BT complex appears to be the resultant M−C bond strength. Calculations by Seigbahn suggest that the M−C bond strengths can be evaluated in terms of ionic contributions to the bond (reflected in atomic charges) and repulsive interactions between metal−carbon and carbon−substituent bonding orbitals. On the basis of these criteria, C_v is expected to form the strongest M−C bond in BT and 3-MeBT while C_a is expected to form the strongest bond in 2-MeBT and η^6-coordinated BT. These results are consistent with the fact that BT and 3-MeBT have been shown to form S−C_v insertion products exclusively while 2-MeBT and η^6-coordinated BT are the only BT species known to form S−C_a metal-inserted products.

In conclusion, it is clear that several components influence insertion selectivities, and each must be considered before predictions about S−C bond activation in BT molecules can be made. While most factors favor insertion into the S−C_v bond (consistent with experiment), subtle structural changes, which affect both steric interactions and metal−carbon bond strengths, can open up possibilities for S−C_a insertion.

Calculational Details

All of the calculations for BT, 2-MeBT, 3-MeBT, $(C_5Me_5)(CO)_2Re(\eta^1\text{-}S\text{-}3\text{-}MeC_8H_5S)$, and all $[(C_5Me_5)Rh(PMe_3)]$-inserted complexes were performed with the Gaussian-94 package.[50]

The geometries of BT, 2-MeBT, and 3-MeBT were calculated at the HF/6-311G* level of theory. All geometrical parameters were optimized using gradient techniques. Electron correlation effects were considered by fully optimizing BT at the level of second-order Møller−Plesset perturbation theory (6-311G* basis set). While both S−C bonds of the heterocycle were slightly shortened compared to the HF/6-311G* geometry, all electronic properties (i.e., charges, bond overlap populations, orbital character, etc.) remained consistent with those at the HF level. Consequently, the HF/6-311G* results were deemed adequate for our purposes.

The geometry of the η^1-S-bound complex $(C_5Me_5)(CO)_2Re(\eta^1\text{-}S\text{-}3\text{-}MeC_8H_5S)$ was also calculated at the HF level of theory. Due to the size of the complex, however, smaller basis sets were employed for the main-group atoms. For S, the standard 6-31G* basis set was used, and for the C, O, and H atoms, the standard 6-31G basis set was used. For the Re atom, the relativistic effective core potential (RECP) of Hay and Wadt,[51] which treats the outermost core orbitals ($5s^25p^6$) as valence, was employed. While use of smaller basis sets was necessary due to the size of the system and limited computational resources, we do not believe that the results concerning the calculated length of the S−C_v bond of the 3-MeBT moiety and the orbital structure of the LUMO and SLUMO of the complex were adversely affected. Complete optimization of $(C_5Me_5)(CO)_2Re(\eta^1\text{-}S\text{-}3\text{-}MeC_8H_5S)$ did reveal a noticeable lengthening of the Re−S bond when compared to the crystallographically determined value, 2.489 vs 2.356 Å. (Lengthening of M−L bonds when performing ab initio HF calculations with RECP's has also been observed in other systems.)[52] We felt that the longer Re−S bond may affect the S−C_v bond distance, and therefore, the geometry of the complex was recalculated after freezing the Re−S bond length to the experimental value. Both calculations produced equivalent S−C_v bond distances of 1.75 Å.

Single-point calculations for the S−C_v metal-inserted product $(C_5Me_5)Rh(PMe_3)(\eta^2\text{-}C,S\text{-}C_8H_6S)$ and both isomers of $(C_5Me_5)Rh(PMe_3)(\eta^2\text{-}C,S\text{-}2\text{-}MeC_8H_5S)$ were calculated at the HF level of theory using structures determined via single-crystal X-ray diffraction.[13,43] We also performed a single-point calculation on the experimentally unknown and, therefore, structurally uncharacterized S−C_a metal-inserted adduct of $(C_5Me_5)Rh(PMe_3)(\eta^2\text{-}C,S\text{-}C_8H_6S)$. The structure of the analogous S−C_a rhodium-inserted 2-MeBT complex was used for the molecular geometry with the methyl group being replaced with a hydrogen atom. The position and length of the new C−H bond was optimized via a molecular mechanics calculation (see below). In all calculations of the rhodium-inserted complexes,

(50) Frisch, M. J.; Trucks, G. W.; Schlegel, H. B.; Gill, P. M. W.; Johnson, B. G.; Robb, M. A.; Cheeseman, J. R.; Keith, T. A.; Petersson, G. A.; Montgomery, J. A.; Raghavachari, K.; Al-Laham, M. A.; Zakrzewski, V. G.; Ortiz, J. V.; Foresman, J. B.; Cioslowski, J.; Stefanov, B. B.; Nanayakkara, A.; Challacombe, M.; Peng, C. Y.; Ayala, P. Y.; Chen, W.; Wong, M. W.; Anders, J. L.; Replogle, E. S.; Gomperts, R.; Martin, R. L.; Fox, D. J.; Binkley, J. S.; Defrees, D. J.; Baker, J.; Stewart, J. P.; Head-Gordon, M.; Gonzales, C.; Pople, J. A. *Gaussian*, Revision D.4; Gaussian, Inc.: Pittsburgh, PA, 1995.

(51) Hay, P. J.; Wadt, W. R. *J. Chem. Phys.* **1985**, *82*, 299−310.

(52) Broo, A. *Int. J. Quantum Chem., Quantum Chem. Symp.* **1996**, *30*, 1331−1343.

Downloaded by CARLI CONSORTIUM on June 30, 2009
Published on July 28, 1998 on http://pubs.acs.org | doi: 10.1021/om980224e

the standard 6-311G* basis set was used for the S, P, C, and H atoms and the RECP, similar to the Re RECP described above, was used for the Rh atom.

Preliminary calculations on the η^6-coordinated BT complexes were carried out using nonempirical, approximate Hartree−Fock, Fenske−Hall molecular orbital calculations.[49] The 1s through *n*d functions for Mn and Ru were generated by a best fit to Herman−Skillman atomic calculations[53] using the method of Bursten, Jensen, and Fenske.[54] The $(n + 1)$s and $(n + 1)$p functions were chosen to have exponents of 2.0 for Mn and 2.2 for Ru. The carbon and sulfur functions were taken from the double-ζ functions of Clementi.[55] The valence p functions were retained as the double-ζ functions, while all the other functions were reduced to single-ζ functions. An exponent of 1.2 was used for hydrogen. Orbital populations, overlap populations, and atomic charges were determined with Mulliken population analyses.[32,33]

Of the three η^6-coordinated BT species studied, only $[(\eta^6\text{-BT})\text{Ru}(\eta^5\text{-}C_5H_5)]^+$ has been structurally characterized via X-ray diffraction.[56] For $[(\eta^6\text{-BT})\text{Mn}(CO)_3]^+$, an idealized structure was generated based on structural data for the η^6-indole analogue.[57] The indole was replaced with the HF/6-311G* BT structure. Similar methodology was employed to generate the $[(\eta^6\text{-BT})\text{Ru}(\eta^6\text{-benzene})]^{2+}$ precursor. In this case, $[(\eta^6\text{-BT})\text{Ru}(\eta^5\text{-}C_5H_5)]^+$ was used as the base structure.

All molecular mechanics calculations were carried out using the 1.02 Universal Force Field[58−60] as implemented through Cerius^2.[61] All energy terms normally active in the force field were included in every calculation. The atoms were typed as follows: manganese, Mn6+2; rhodium, Rh6+3; sulfur, S_2; phosphorus, P_3; carbonyl oxygen, O_1; carbonyl carbon, C_1; thiophene carbon, C_2 or C_R; alkyl carbon, C_3; hydrogen, H_. For the $S-C_a$ $[(C_5Me_5)\text{Rh}(PMe_3)]$-inserted BT complex (derived from the 2-MeBT analogue), only the substituted H atom was allowed to minimize. For the bimetallic manganese system, the tricarbonyl manganese moiety and the arene ring of the heterocycle were frozen while all other atoms were minimized. This allowed for determination of steric factors influencing the inserted $[\text{Mn}(CO)_4]$ fragment.

Acknowledgment. Financial support of this research by the National Science Foundation (Grant No. CHE-9421784) is greatly appreciated. S.R. also thanks NSF REU (Grant No. CHE-9424241) for support.

OM980224E

(53) Herman, F.; Skillman, S. *Atomic Structure Calculations*; Prentice Hall: Englewood Cliffs, NJ, 1963.
(54) Bursten, B. E.; Jensen, J. R.; Fenske, R. F. *J. Chem. Phys.* **1978**, *68*, 3320−3321.
(55) Clementi, E. *J. Chem. Phys.* **1964**, *40*, 1944−1945.
(56) Huckett, S. C.; Miller, L. L.; Jacobson, R. A.; Angelici, R. J. *Organometallics* **1988**, *7*, 686−691.
(57) Ryan, W. J.; Peterson, P. E.; Cao, Y.; Williard, P. G.; Sweigart, D. A.; Baer, C. D.; Thompson, C. F.; Chung, Y. K.; Chung, T.-M. *Inorg. Chim. Acta* **1993**, *211*, 1−3.
(58) Casewit, C. J.; Rappé, A. K.; Colwell, K. S.; Goddard, W. A., III; Skiff, W. M. *J. Am. Chem. Soc.* **1992**, *114*, 10024−10035.
(59) Casewit, C. J.; Rappé, A. K.; Colwell, K. S. *J. Am. Chem. Soc.* **1992**, *114*, 10035−10045.
(60) Casewit, C. J.; Rappé, A. K.; Colwell, K. S. *J. Am. Chem. Soc.* **1992**, *114*, 10046−10053.
(61) *Cerius^2*, Version 3.0; Molecular Simulations Inc.: San Diego, CA, 1996.

Downloaded by CARLI CONSORTIUM on June 30, 2009
Published on July 28, 1998 on http://pubs.acs.org | doi: 10.1021/om980224e